Separation of the polymer matrix and the fibrous reinforcement during compression moulding of Glass Mat Thermoplastics (GMT)

Laurent Orgéas[1], Pierre J.J. Dumont[2], Véronique Michaud[3], Denis Favier[1]

[1]Laboratoire Sols-Solides-Structures-Risques (3SR), CNRS - Université de Grenoble (INPG-UJF)
BP 53, 38041 Grenoble cedex 9, France
URL: www.3s-r.hmg.inpg.fr/3sr/, e-mail: Laurent.Orgeas@hmg.inpg.fr, Denis. Favier@hmg.inpg.fr
[2]Laboratoire de Génie des Procédés Papetiers (LGP2), CNRS - INPG
BP 65, 461 rue de la Papeterie, 38402 Saint-Martin-d'Hères cedex, France
URL: www.efpg.inpg.fr/, e-mail: Pierre.Dumont@efpg.inpg.fr
[3]Laboratoire de Technologie des Composites et Polymères (LTC), Ecole Polytechnique Fédérale de Lausanne (EPFL), Station 12, CH-1015 Lausanne, Switzerland
URL: www.epfl.ch, e-mail: Veronique.Michaud@epfl.ch

ABSTRACT: Homogeneous plane strain compression tests were performed on standard industrial GMT composites using a channel mould at 200^oC. A charring and weighting technique was used to determine the fibre concentration after the compression experiments. Experimental results emphasise the influences of the initial length of samples, the compression elongation and axial strain rate on the fibre-matrix separation phenomenon.

KEYWORDS: Rheology, Fibre-Matrix Separation, Compression, GMT, Short Fibre Polymer Composites

1 INTRODUCTION

Compression moulded composites such as Glass Mat Thermoplastics (GMT) are widely used in the automotive industry. These materials are made up of a thermoplastic matrix reinforced with needled glass fibre mats. During their forming process, *i.e.* compression moulding, migration of the liquid thermoplastic matrix through the deforming fibrous reinforcement may occur [5, 2]. Similar fibre-matrix separation has also been observed during the compression of Sheet Moulding Compounds (SMC) [4] or during the injection moulding of short fibre reinforced thermoplastic polymers [1]. This phenomenon leads to undesirable microstructure gradients within produced parts, that strongly affect their final properties. Factors influencing fibre-matrix separation are still not very well understood. The aim of the present work is to bring experimental results to better identify these factors in the case of the compression of GMT. For that purpose, homogeneous plane strain compression tests were performed on standard industrial GMT using a channel mould at a constant temperature of 200^oC. A charring and weighting technique was used to determine the fibre concentration along compressed samples. The influence of various parameters including the initial length of the samples, the compression strain and the axial strain rate was explored. This allows to establish some phenomenological rules that govern fibre-matrix separation.

2 MATERIALS

GMT plates of initial thickness $h_0 \approx 5$ mm were supplied by Quadrant AG (Switzerland). They were made of fibre bundle mats impregnated by a polypropylene matrix. The glass fibre bundle mats consisted of in-plane randomly oriented chopped fibre bundles that were needled in the out-of-plane direction $\mathbf{e}_3$. Bundles were composed of approximately 200 glass fibres of diameter 15 μm. Their length was 50 mm and their elliptical cross section exhibited major and minor axes close to 80 and 400 μm, respectively. The initial mass fraction of fibres $f_0 = 0.33 \pm 0.01$ was determined according to the procedure described in the next section. The rheology of the polymer matrix at 200^oC was analysed with a parallel plates rheometer (for shear strain rates $\dot{\gamma}$ ranging from 10^{-3} to 10 s^{-1}) and a capillary rheometer (for shear rates ranging from 10 to 10^4 s^{-1}). As shown in

the graph plotted in figure 1, the steady state shear viscosity μ of the matrix exhibits non-Newtonian effects which are well-captured by the following Carreau-Yasuda model:

$$\mu = \mu_0(1 + (\dot{\gamma}/\dot{\gamma}_c)^a)^{(n-1)/a} \quad (1)$$

where the Newtonian viscosity μ_0, the power-law exponent n, the characteristic shear rate $\dot{\gamma}_c$ and the curvature parameter a were set to 160 Pa s, 0.36, 200 s^{-1} and 1, respectively.

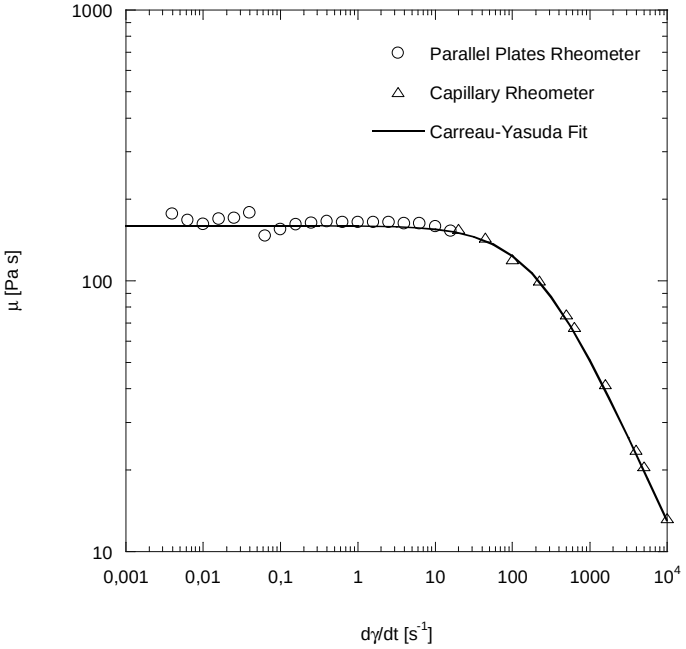

Figure 1: Evolution of the shear viscosity μ of the PP matrix with the shear strain rate $\dot{\gamma}$ at 200^{o}C.

3 EXPERIMENTAL PROCEDURE

Rectangular samples were cut from the moulded plates with two different initial lengths L_0 ($\mathbf{e}_1$ direction), i.e. 80 and 160 mm, and a width $l_0 = 80$ mm ($\mathbf{e}_2$ direction). These samples were compressed inside a rectangular channel of width $l_0 = 80$ mm, using a specially designed plane strain compression rheometer [3]. This rheometer was mounted on a hydraulic press (Interlaken Tech. Corp. series 3300) with a 100 kN load cell equipped with an oven. The testing temperature of the experiments was set to 200 ± 1^oC.

In order to ensure a good homogeneity of the sample deformation, samples were coated with silicone grease prior to the tests. During the experiments, the current height h of the sample as well as the current axial compression force F ($\mathbf{e}_3$ direction) were simultaneously recorded. This allows to determine the axial elongation (stretch) $\lambda = h/h_0$ as well as the nominal axial stress $\Sigma = |F|/l_0L_0$. Notice that tests were performed at constant axial velocity v until an elongation λ_f, and that the initial axial strain rate $D_0 = |v|/h_0$ was varied from 10^{-4} to 10 s^{-1}. At the end of the tests, deformed samples were cooled to room temperature (20^{o}C). Therefrom, parallel strips (width l_0 and length $\Delta L \approx 10$ mm) were (i) cut from the samples along the flow direction $\mathbf{e}_1$, (ii) weighted, (iii) charred into a furnace at 500^{o}C for 30 min, and (iv) weighted again. This allowed to estimate the mass fraction of fibres f along the flow direction $\mathbf{e}_1$ of the deformed samples.

4 RESULTS

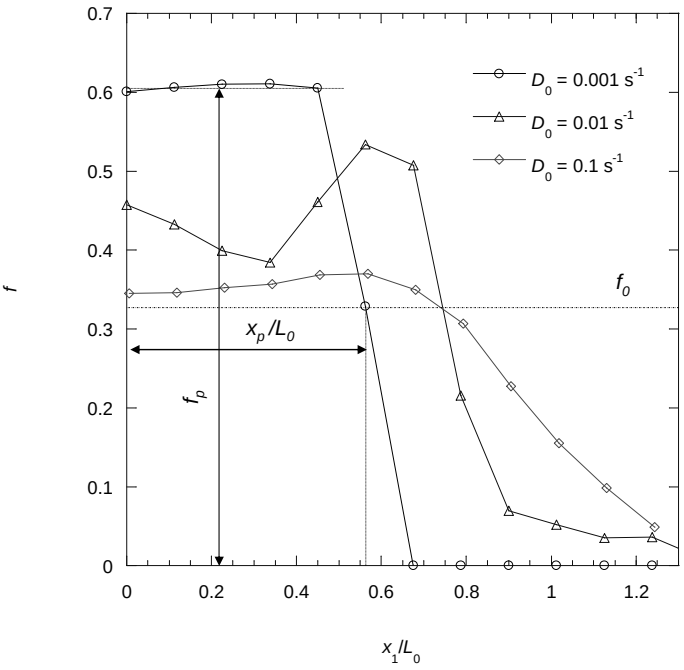

Figure 2: Evolution of the fibre content f along the normalised abscissa x_1/L_0 at various initial strain rates D_0 (compression elongation $\lambda_f = 0.4$, initial sample length $L_0 = 80$ mm).

The graph sketched in figure 2 gives three typical curves showing the evolution of the fibre content f along the normalised abscissa x_1/L_0 obtained from samples of initial length $L_0 = 80$ mm that have been deformed at a compression elongation $\lambda_f = 0.4$ ($x_1 = 0$ corresponding to the centre of samples). Whatever the imposed axial strain rate D_0, this figure reveals heterogeneous fibre contents within deformed

samples: migration of the polymer matrix through the fibrous network has occurred during the experiments.

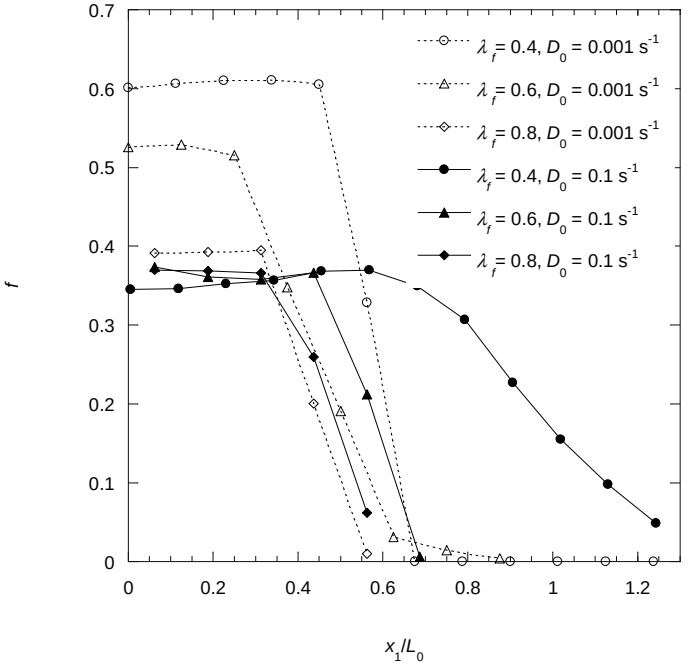

Figure 3: Evolution of the fibre content f along the normalised abscissa x_1/L_0 for various compression elongations λ_f and various strain rates D_0 (initial sample length $L_0 = 80$ mm).

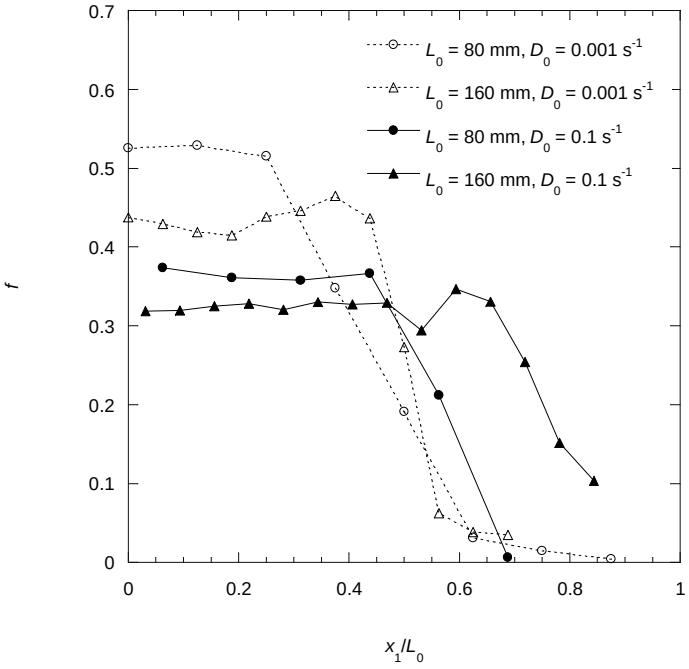

Figure 4: Evolution of the fibre content f along the normalised abscissa x_1/L_0 for various initial sample lengths L_0 and various strain rates D_0 (compression elongation $\lambda_f = 0.6$).

The influence of the elongation λ_f on the fibre-matrix separation is emphasised in figure 3, where the evolution of f along the normalised abscissa x_1/L_0 is reported for samples deformed at different values of λ_f (two axial strain rates D_0, initial length $L_0 = 80$ mm).

Lastly, we report in figure 4 the evolution of f with x_1/L_0 for samples displaying different initial lengths L_0 and deformed at two axial strain rates D_0 ($\lambda_f = 0.6$).

As shown from the example given in figure 2, three zones are systematically observed. In the centre of samples, f exhibits a plateau characterised by a more or less constant fibre content f_p (see figure 2), which is higher than f_0. Near the free surfaces of samples, f is much lower than f_p and f_0. The transition zone in which f rapidly decreases is located between the two previous regions at a normalised abscissa x_p/L_0 (see figure 2). Besides, the above results allow to establish the following phenomenological rules:

(a) the lower the imposed strain rate D_0, the higher the fibre-matrix separation: for example, f_p is much higher for tests performed at $D_0 = 0.001$ s^{-1} than for tests performed at $D_0 = 0.1$ s^{-1}, as evident from figure 2.

(b) the lower the compression elongation λ_f, the higher the fibre-matrix separation. At high strain rates, this is revealed by the increase of the width of the transition zone as λ_f diminishes (see figure 3). At low strain rates, fibre-matrix separation is underlined by the strong increase of f_p with λ_f (see figure 3).

(c) the lower the initial length of samples L_0, the higher the fibre-matrix separation. As shown from figure 4, this has been observed at different axial strain rates D_0: f_p is systematically higher for smaller samples.

5 DISCUSSION, CONCLUDING REMARKS

Results obtained in the previous section have shown that during the compression of GMT, migration of the polymer matrix through the deforming fibrous network is a phenomenon which systematically occurs. It has been shown here that its magnitude depends on processing conditions such as the initial sample length, the compression elongation and the axial strain rate. Among them, the role of the axial strain rate seems to be predominant. To illustrate this, evolutions of f_p and x_p/L_0 at $\lambda_f = 0.4$ and as functions of the imposed initial axial strain rate D_0 have

been reported in the graph of figure 5. We have also reported in this graph stress levels Σ recorded during compression experiments at $\lambda = 0.8$. This figure brings up the following comments:

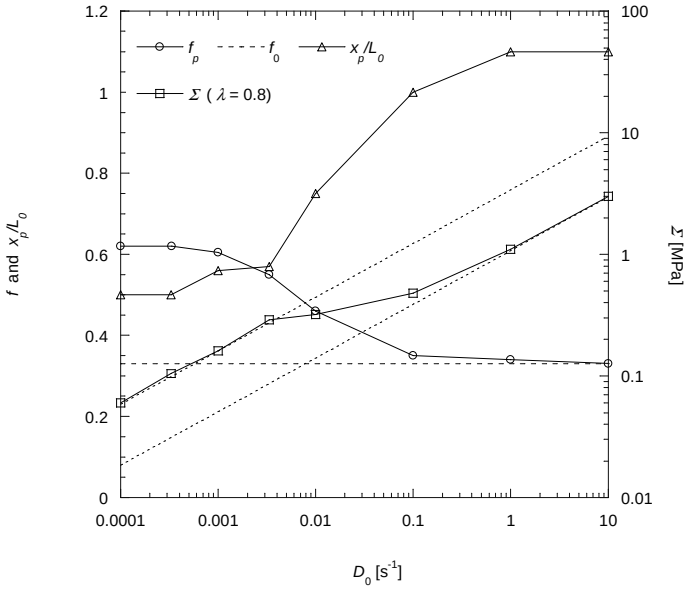

Figure 5: Evolution of f_p, x_p/L_0 and $\Sigma(\lambda = 0.8)$ with D_0 (initial sample length $L_0 = 80$mm)).

(a) For low values of D_0, *i.e.* when $D_0 \leq 0.001$ s^{-1}, fibre-matrix separation is pronounced: f_p is much higher than f_0 and x_p/L_0 is very close to 0.5, *i.e.* close to its initial value before compression: fibrous networks have been compressed in the $\mathbf{e}_3$ direction without flowing in the $\mathbf{e}_1$ one (nearly oedometric compaction). Hence, the rheology of GMT in this strain rate range is that of a two-phase medium ("consolidation" regime): (i) the interstitial pressure within the polymer matrix is sufficiently low so that fibre bundles remain entangled and needled and are severely compressed , (ii) the interstitial pressure gradient from the centre of samples to their free surface is high enough to induce the migration of the non-Newtonian polymer matrix through the fibrous networks.

(b) For high values of D_0, *i.e.* when $D_0 \geq 0.1$ s^{-1}, fibre-matrix separation is much less pronounced. Indeed, f_p is closer to f_0 and x_p/L_0 reaches values equal to 1.1, showing that fibrous networks have flowed in the $\mathbf{e}_1$ direction during their compression. The rheology of GMT in this strain rate range tends to that of a one-phase medium ("liquefaction" regime). This also suggests that (i) the interstitial pressure within the polymer matrix is sufficiently high to induce the disentanglement and the relative motion of fibre bundles, (ii) the interstitial pressure gradient is not high enough to induce significant flow of the polymer matrix through fibres.

(c) For values of D_0 between 0.001 s^{-1} and 0.1 s^{-1}, a transition zone between the two previous ones is observed.

(d) Within the "liquefaction" or the "consolidation" regimes, stress levels follow power-laws with an identical power-law exponent of 0.4 (see the two parallel dotted lines sketched in figure 5), which is very close to that obtained for the polymer matrix above 100 s^{-1} (see figure 1). Within the "consolidation" regime, this suggests that deformation mechanisms occurring at the fibre scale are mainly ruled (i) by the flow of the non-Newtonian polymer through fibre bundles, (ii) by non-Newtonian viscous friction forces at bundle-bundle contacts, the last mechanism being the only one within the "liquefaction" regime.

ACKNOWLEDGEMENT

The authors wish to thank the company Quadrant for supplying the GMT and the GDRE "HETerogeneous MATerials" for its financial support.

REFERENCES

[1] F. Danes, B. Garnier, T. Dupuis, P. Lerendu, and T.-P. Nguyen. Non-uniformity of the filler concentration and of the transverse thermal and electrical conductivities of filled polymer plates. *Compos. Sci. Technol.*, 65:945–951, 2005.

[2] P. Dumont, L. Orgéas, C. Servais, V. Michaud, D. Favier, and J.A.E. Manson. Influence of material and process parameters on segregation phenomena during compression molding of GMT. In The Pub. House of the Rom. Acad., editor, *Proc. Of 8th Int. ESAFORM Conf. On Material Forming*, pages 975–78, The Pub. House of the Rom. Acad, 2005.

[3] P. Dumont, J.-P. Vassal, L. Orgéas, V. Michaud, D. Favier, and J.A.-E. Månson. Processing, characterization and rheology of transparent concentrated fibre bundle suspensions. *Rheol. Acta*, 46:639–641, 2007.

[4] T.H. Le, P.J.J. Dumont, L. Orgéas, D. Favier, L. Salvo, and E. Boller. X-ray phase contrast microtomography for the analysis of the fibrous microstructure of SMC composites. *Compos. Part A*, 39:91–103, 2008.

[5] Y. Yagushi, H. Hojo, D. G. Lee, and E. G. Kim. Measurement of planar orientation of fibers for reinforced thermoplastic using image processing. *Int. Polymer Processing*, 3:262–269, 1995.